Heteroatom Chemistry
Volume 18, Number 2, 2007

Dynamic Aspects of Hypervalent Compounds Effected by the Formation of Three Center-Four Electron Bond in Heteroatoms

Kin-ya Akiba[1] and Yohsuke Yamamoto[2]

[1]*Advanced Research Institute for Science and Engineering, Waseda University, 3-4-1 Ohkubo Shinjuku-ku, Tokyo 169-8555, Japan*

[2]*Department of Chemistry, Graduate School of Science, Hiroshima University, 1-3-1 Kagamiyama, Higashi-Hiroshima 739-8526, Japan*

Received 7 September 2005; revised 25 October 2005

ABSTRACT: *Hypervalent bond (three center-four electron bond: 3c-4e) is the central feature of the structure and reactivity of hypervalent compounds. The S—S—S bond of thiathiophthene, the so-called no-bond resonance compound, is realized as one of the examples of 3c-4e bond centered at the sulfur atom (10-S-3). A variety of reactions such as cycloaddition-elimination, bond-switching rearrangement, and bond-switching equilibration of sulfur-containing heterocycles are exemplified to proceed through the presence of hypervalent 10-S-3 species. In the transition state of edge inversion, it is predicted that a vacant p-type orbital is perpendicular to the square planar species. Antimony(III) and bismuth(III) compounds bearing a bidentate Martin ligand and a phenyl, or 2-dimethylaminomethylphenyl, or 2,6-bis(dimethylaminomethyl)phenyl group were prepared. The rates of inversion of these compounds at the central atom of Sb or Bi were accelerated significantly by the coordination of the dimethylamino group and also of pyridine from the solvent, where 3c-4e bond is formed by the coordination to stabilize the transition state. Finally, the presence of rapid bond-switching equilibration between N—B···N bond of 1,8-bis(dimethylamino)-9-(substituted)borylanthracenes was shown to proceed through 10-B-5 species at the transition state. It is concluded that the bond-switching equilibration takes place as a piston rod in the range of 1.32 Å.* © 2007 Wiley Periodicals, Inc. Heteroatom Chem 18:161–175, 2007; Published online in Wiley InterScience (www.interscience.wiley.com). DOI 10.1002/hc.20326

Correspondence to: Kin-ya Akiba; e-mail: akibaky@waseda.jp.

INTRODUCTION

The most popular and well-known weak covalent interaction is the hydrogen bond, which is made of a covalent X—H bond and a lone-pair electrons of X atom (X—H···X). The formation of this bond is also realized by the interaction of lone-pair electrons on each X atom and a proton as the central atom (X: H^+ :X). This is one of the examples of three-center four-electron bond (3c-4e bond). The 3c-4e bond is now established as the hypervalent bond [1], which is widely seen as apical bonds of pentacoordinate (or pseudopentacoordinate) hypervalent compounds such as silicon [2], phosphorus [3], sulfur [4], and iodine [5]. The shape of these molecules is essentially trigonal bipyramid (TBP) and the central atom (X) is sp^2 hybridized, and the three bonds are equatorial bonds binding three ligands or substituents and there is a p-orbital that is perpendicular to the equatorial plane. This orbital is used to keep two substituents as apical ligands forming 3c-4e bond.

As early as 1951, Pimental and Rundle independently proposed the idea of 3c-4e bond in order to describe the easy formation and excellent stability of triiodie ion and others by employing molecular orbital theory [6]. The idea was not accepted by the chemical community soon; however, the general concept of hypervalent molecules was established by Musher in 1969, i.e., hypervalent molecules are ions or molecules of group 15–18 elements (main group elements) which bear more electrons than the octet (nine or more) within a valence shell [7]. In order to formally admit extra electrons over Lewis octet on the central atom of main group elements, highly ionic (50% or more) orbitals modifying the basic idea of covalent bond is required. This is in accord with the fundamental character of 3c-4e bond, one pair of electrons is delocalized to the two ligands (substituents) resulting in the charge distribution of almost −0.5 charge on each ligand and almost +1.0 charge on the central atom. Owing to the rapid progress of computer and theoretical calculations [8], the idea of 3c-4e bond to admit extra electrons over octet on main group elements has become supported as opposed to d-orbital contribution and is presently accepted as a hypervalent bond.

To conceptually create a 3c-4e bond (apical bond) of pentacoordinate molecules, three models can be considered: (i) add two free radicals to coordinate with a pair of unshared electrons in a p-orbital, (ii) add two pairs of unshared electrons (nucleophiles) to coordinate with a vacant p-orbital, or (iii) add a pair of unshared electrons to coordinate with the σ^* orbital of an X—Z bond in a cationic or neutral molecule. When X is a carbon in a neutral molecule, model (iii) corresponds to the formation of the transition state (TS) of the S_N2 reaction as shown in Scheme 1.

RING TRANSFORMATION AND BOND SWITCHING AT 10-S-3 SULFURANES

The fundamental electronic structure of 3-coordinate sulfur, 10-S-3 species, is shown by the valence bond method as **1**. The central sulfur atom bears two unshared electron pairs and one S—A bond (sp^2 bond) in a plane, and the 3c-4e bond is perpendicular to the plane, which consists of apical bonds (B—S—B) in order to keep two ligands.

Such a bond is stabilized when electron-withdrawing ligands (substituents) occupy the apical position, but on the other hand the bond between S and B becomes longer and weaker according to the increase in electronegativity of the substituent (B). These characteristics, if based on superficial understanding, seem to be contradictory to the stability of the molecule; however, it is the case.

One of the well-known examples to show this peculiar character is the so-called thiathiophthene **2**, i.e., 1,6,6a-trithia(6a-S^{IV})pentalene **2c** (Scheme 2) [9]. X-ray analysis of **2** shows (i) the molecule is planar and symmetric with respect to the S(6a)-C(3a) axis, and the three sulfur atoms are linear, (ii) the S—S bond length is 2.363 Å and is longer than the sum of the covalent radii (2.08 Å) and shorter than the sum of van der Waals radii (3.70 Å), (iii) the bond

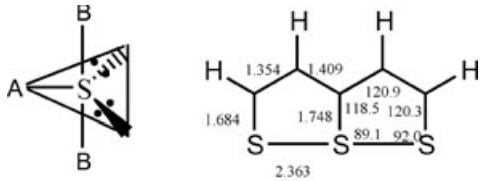

1 **2**

SCHEME 2 TBP structure of 10-S-3 and trithiapentalene.

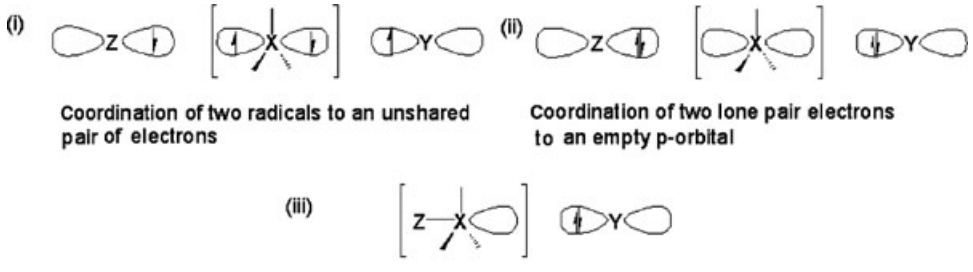

SCHEME 1 Conceptual models of the three-center four-electron (3c-4e) bond of pentacoordinate molecules.

S(6a)-C(3a) (1.748 Å) is longer than the bond S(1)–C(2) (1.684 Å), (iv) the bond C(2)–C(3) (1.354 Å) is shorter than the bond C(3)–C(3a) (1.409 Å).

The description of **2c**, which has a double bond between S(6a)-C(3a) and a lone-pair electrons in the molecular plane, is not consistent especially with the fact (iii) and also cannot show the fundamental character of the presence of elongated S—S bond ((i) and (ii)). In order to rationalize this, the idea of no bond resonance was proposed, showing that the bond order between the sulfur is 0.5 [10]. When there is a substituent(s) on the carbon skeleton of **2**, electronic and steric effects appear on the S—S bond lengths rendering the molecular frame unsymmetrical, whereas that of S(6a)-C(3a) remains almost constant. The S–S bond length varies between 2.20 and 2.50 Å by X-ray analysis depending on the substituent(s). The unsymmetrical nature of the molecule, however, cannot be seen in solution; hence, the S—S bond is weak and susceptible to electronic effect and there may be rapid bond switching in the solution. The character is most accurately described by 3c-4e bond (**2d**; 10-S-3), the two lone-pair electrons are up and down from the molecular plane, and formal plus and minus charges are located at C_{3a} and S_{6a} (Scheme 3).

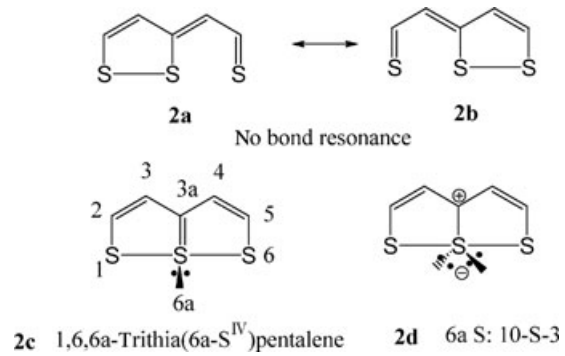

SCHEME 3 Structure of thiathiophtene **2**.

When 10-S-3 species is invoked as an intermediate or the transition state by valence expansion from 8-S-2 to 10-S-3, a variety of ring transformation and/or bond switching can take place according to the structure of the intermediate 10-S-3. First, several examples are cited from the literature as shown in Scheme 4 [11–13].

For the reaction of thiadiazolines and activated acetylenes, it was shown that the products obtained were totally different according to the nature of the substituent(s) and of the position of heteroatoms in the starting five-membered ring. For example, 5-imino-1,2,4-thiadiazoline (**3**) reacted with activated acetylenes to give the corresponding 2-aminothiadiazole and nitrile by addition-elimination [14]. On the other hand, 2-iminothiazoline (**4**) gave simple addition products (Scheme 5).

This result can be understood by the difference in stability of the 3c-4e bond assumed in the intermediate (**A** or **C**). In the latter case (**C**) the 3c-4e bond consists of C—S—C, and in the former (**A**) it is made of N—S—C. The 3c-4e bond in the former (**A**) containing the more electronegative nitrogen atom should be more stable compared with **C**, hence the reaction through **A** is preferred. The reaction path involving **C** may surely be energetically unfavorable, thus the reaction proceeded through the zwitterion **B** to give an addition product.

Then, the reactions of 3-substituted 2-imino-1,3,4-thiadiazolines (**5** and **6**) with activated acetylenes were tried to see the difference in nature of the intermediate (**D** or **E**), where the

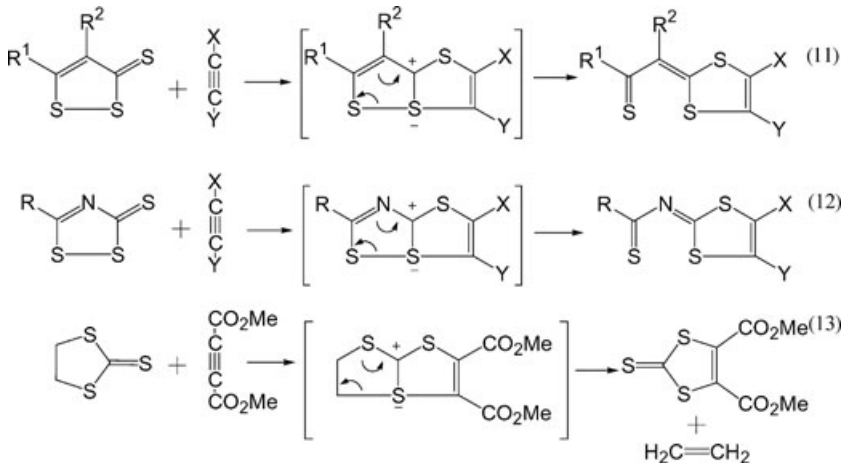

SCHEME 4 Selected examples of bond switching at 10-S-3 from the literature.

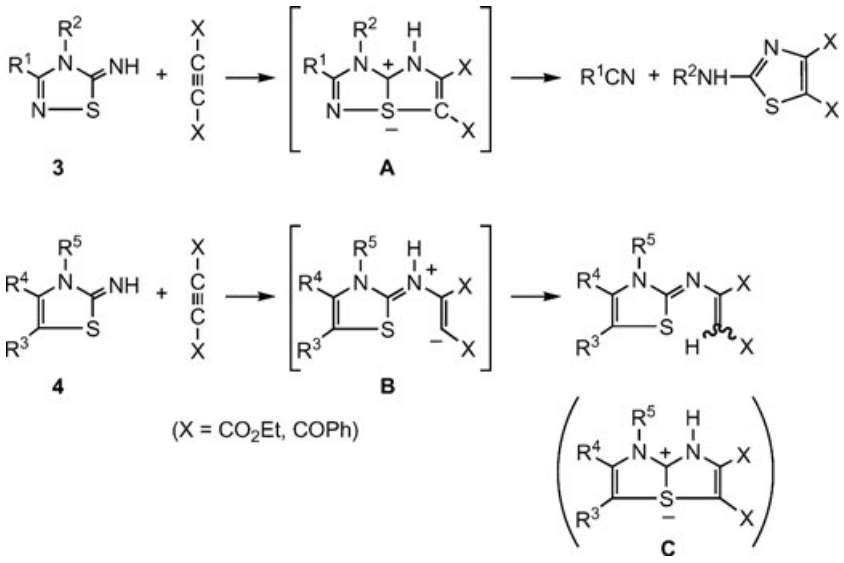

SCHEME 5 Reactions of iminothiazolines with activated acetylenes.

electron-withdrawing ability of the 3c-4e bond is adjusted by a phenyl or a benzoyl group at C-5 [15]. The reaction of **5** with activated acetylenes gave simply the addition product. However, **6** reacted with the same acetylenes in a competitive manner to afford a simple addition product via a zwitterion intermediate (**F**) and addition-elimination product via a 10-S-3 sulfurane intermediate (**E**). The ratio of the competition depended very much on the polarity of solvents. The competition was observed even in alcohols, thus certifying that the two paths are really competitive as shown in Scheme 6 [14,15].

A reaction of **3** with nitriles in the presence of aluminum trichloride or with the corresponding imidates afforded **7**, where ring transformation took place induced by prototropy to give an aromatic thiadiazole ring [16]. Bond-switching equilibration, i.e., ring transformation equilibrium, was observed when the same skeleton (**9-α** and **9-β**) was obtained by ring transformation [17].

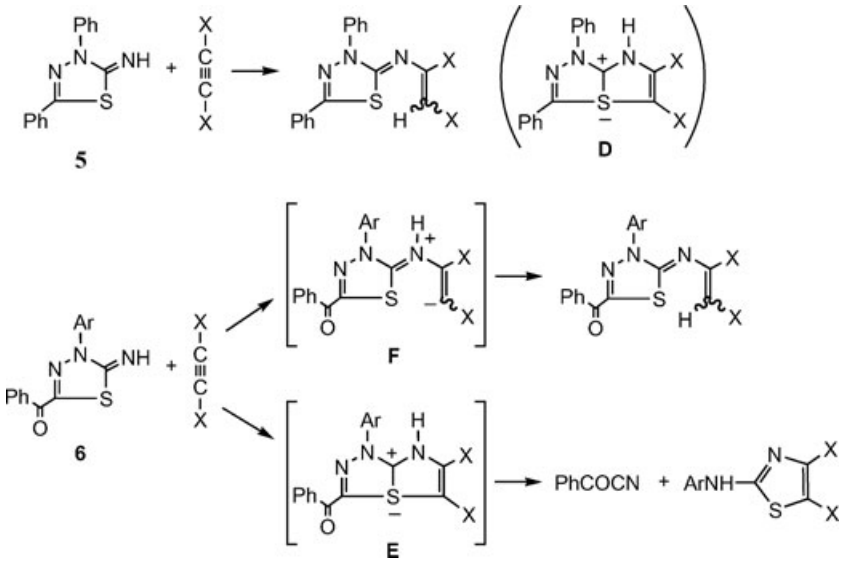

SCHEME 6 Reactions of 2-imino-1,3,4-thiadiazolines with activated acetylenes.

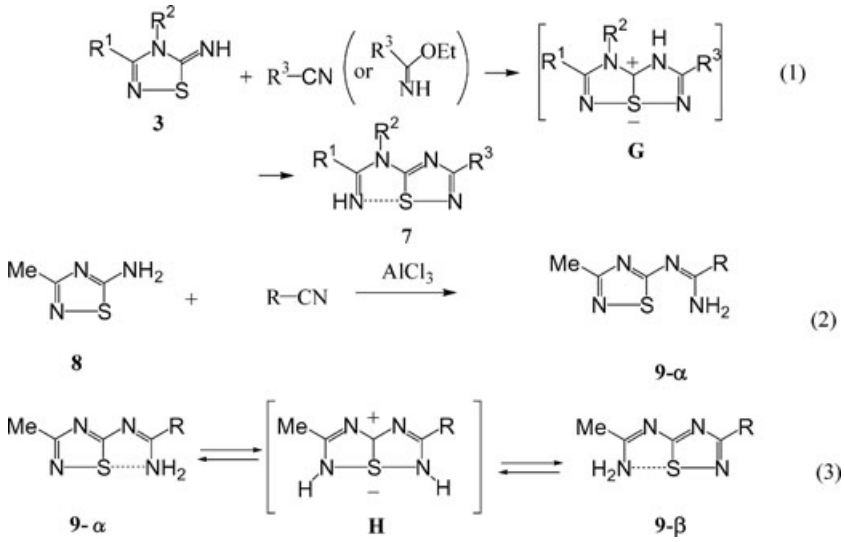

Actually, the same mixture of **9** was obtained when **9-α** and **9-β** were prepared by independent routes, i.e., reaction of 5-amino-3-methyl-1,2,4-thiadiazole (**8**) and nitriles to give **9α** and the same type of reaction with 5-amino-3*R*-1,2,4-thiadiazole and acetonitrile to give **9β**. The equilibrium ratios in solution ($CDCl_3$) are as follows:

9, R, **β**/**α**; **9a**, Me, 1.00; **9b**, CH_2Cl, 2.14; **9c**, CH_2Me, 1.68;

9d, *t*-Bu, 8.57; **9e**, C_6H_5, 14.5; **9f**, *p*-ClC_6H_4, ~50

ORTEP drawings of **7a** and **9b** are shown in Scheme 7. Only **9b-β** was obtained as crystals, and the amidino group of **9b-β** is rotated that to be stabilized by an intramolecular hydrogen bond. These kinds of ring transformation could not be observed for the corresponding oxygen analogue at all; **10b-α** and **10b-β** were prepared as independent molecules.

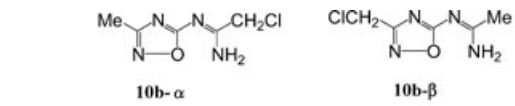

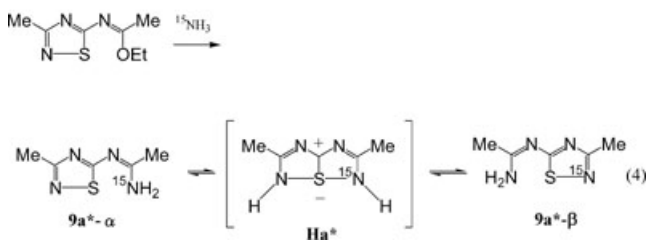

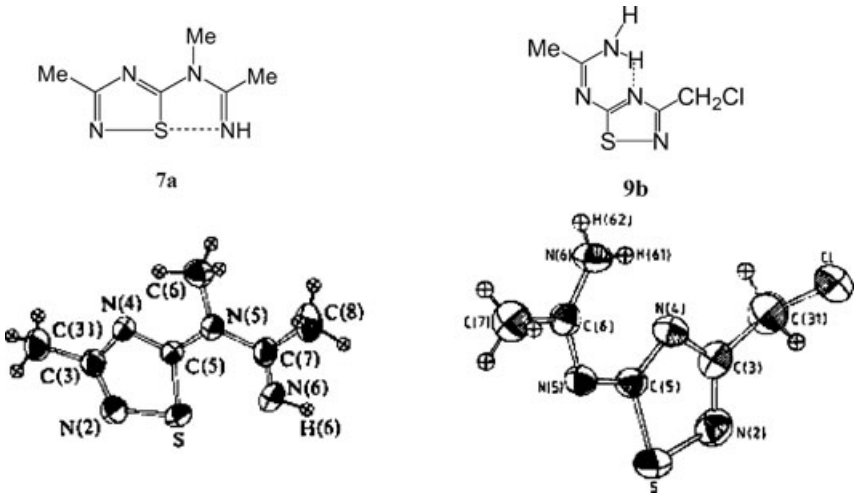

SCHEME 7 ORTEP drawing of **7a** and **9b** (CH_3-CH_2Cl).

The rate of ring transformation (3) was rapid in the solution and **9-α** and **9-β** could not be separated, but it was too slow to measure by ^{1}H NMR. The presence of equilibration was confirmed by preparing ^{15}N-labeled **9a*-α**, where **9a*-α** and **9a*-β** were observed in 1.0:1.0 ratio by ^{15}N NMR. The rate of ring transformation of symmetrical **9a*** was enormously accelerated by acid, and that of monoprotonated species was measured at low temperatures. In the presence of excess TFA, only monoprotonated species **9a*-α-H$^+$-*i*** is observed in CD_3OD at about 0°C. Protonation takes place at the amidino nitrogen and not at the aromatic nitrogen because pK_a of **9a** was measured to be 4.78 + 0.02. The rate was the same even with large excess of TFA. These facts suggest that the rate-determining step deals with the ring transformation of monoprotonated **9a*-α-H$^+$-*ii*** and **9a*-β-H$^+$-*ii***, effected by S_N2 type attack by the NH_2 group to the sulfur. Activation parameters were $\Delta G^{\ddagger}_{273} = 14.8 \pm 0.2$ kcal/mol, $\Delta H^{\ddagger} = 11.6 \pm 1.0$ kcal/mol, $\Delta S^{\ddagger} = -12 \pm 3$ eu, and the rate was $k_{273} = 9\ s^{-1}$ in CD_3OD in the presence of 1.23 equivalent of TFA (Scheme 8) [18,19].

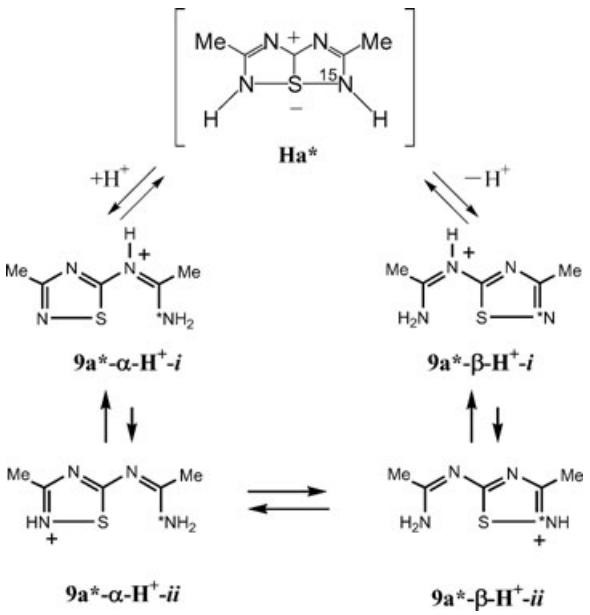

SCHEME 8 Acceleration of ring transformation by protonation of **9a***.

By employing a silyl group shift and desilylation, 5-(2-aminovinyl)isothiazole **11*-α**, which has ^{15}N at the aminovinyl group, was prepared in a pure form (Scheme 9) [20]. When **11*-α** was heated in C_6D_6 and DMSO-d_6 at 60°C, the equilibrium mixture of **11*-α** and **11*-β** was obtained, where hypervalent sulfurane **I** was invoked as an intermediate. The rate of equilibration from **11*-α** to **11*-β** followed exactly the first-order rate in the presence of equilibration: the rate was faster in benzene-d_6 than in DMSO-d_6. Deuterium, which was initially on nitrogen, was gradually distributed to the vinyl and isothiazolyl hydrogen. Based on these findings, it was concluded that the ring transformation of **11** is effected by sigmatropy of hydrogen through a symmetric intermediate **I** as 10-S-3 sulfurane, where the hypervalent bond is not so strongly polarized according to the symmetrical structure. Kinetic parameters of equilibration of **11a** (Ar^1 = Ar^2 = *p*-ClC_6H_4) in benzene-d_6 were also obtained as $\Delta G^{\ddagger}_{298} = 24.4 \pm 0.8$ kcal/mol, $\Delta H^{\ddagger} = 12.2 \pm 0.2$ kcal/mol, $\Delta S^{\ddagger} = -41.0 \pm 0.5$ eu, and $k_{298} = 6.21 \times 10^{-6}\ s^{-1}$.

The structure of the intermediate **I** can be assigned as in Scheme 9, where the S—N bond length should approximately be 1.90 Å, based on the X-ray result of the corresponding compounds of **12** and **13** [21]. As the S—N bond length of isothiazole is known to be 1.67 Å, the S···N bond length of **11** is assigned as 2.50 Å in comparison to similar structures. Then the N—S···N bond (4.17 Å) of **11-α** contracts to become an intermediate **I** (3.80 Å), and then becomes **11-β̃**.

Hence, the central sulfur atom switches back and forth at least in the range of 0.46 Å (3.80−2×1.67) along the hypervalent N—S—N bond, that is bond switching at 10-S-3 sulfurane as shown in Scheme 10. From such results, the flexibility and weakness of 3c-4e bond of 10-S-3 sulfuranes are demonstrated.

In order to determine the bond energy of hypervalent N—S—N bond, a sulfurane fused with two pyrimidine rings (**14**) was prepared and the structure

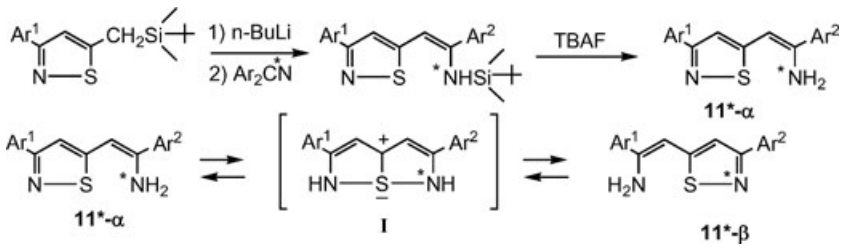

SCHEME 9 Synthesis and equilibration of **11**.

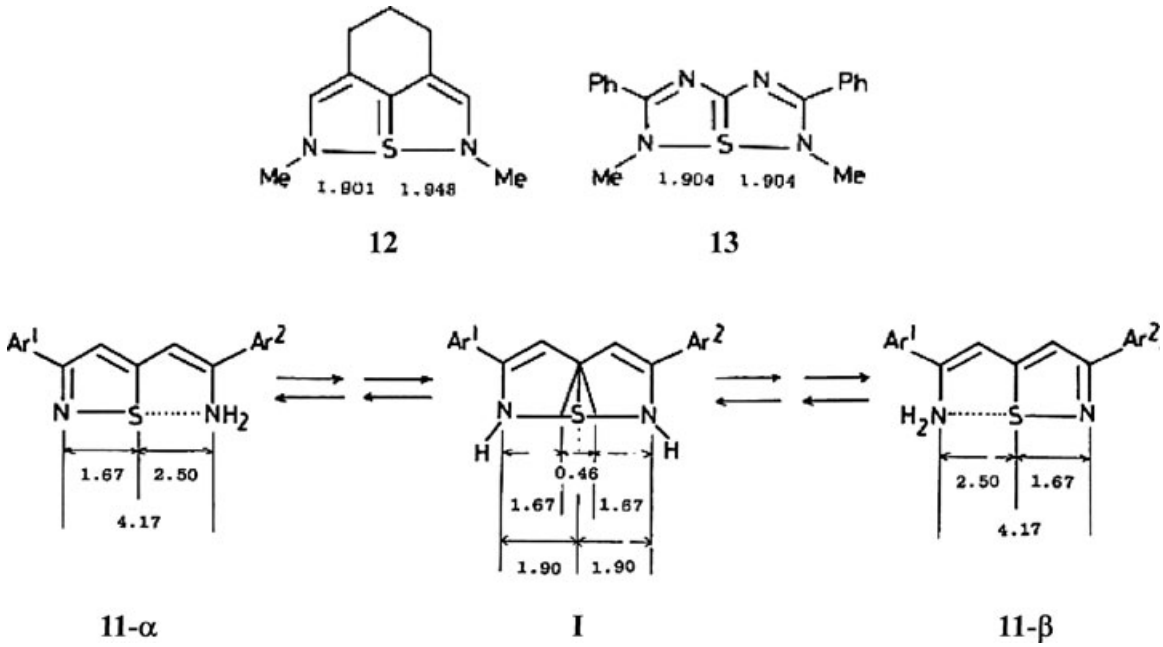

SCHEME 10 The structure of intermediate **I** and bond switching at 10-S-3 sulfuranes.

was determined to be planar by X-ray analysis [22,23]. As there are two nitrogens in a pyrimidine ring, new hypervalent N^2—S bond is formed by the rotation of the pyrimidine ring when the original N^1—S bond is cleaved, as shown in Scheme 11. The bond energy of the hypervalent N—S—N bond can be obtained approximately by measuring the rates of rotation of the two methyl groups (Me^1 and Me^2) of the pyrimidine ring by temperature-dependent measurement of ^{1}H NMR. The apparent S—N bond energy of **14** was obtained as $\Delta G^{\ddagger}_{298} = 16.6$ kcal/mol, $\Delta H^{\ddagger} = 15.9 \pm 1.1$ kcal/mol, and $\Delta S^{\ddagger} = -2.4 \pm 3.4$ eu as shown in Table 1. However, these values should involve the barrier to rotation of the pyrimidine ring which is in conjugation to the other part, hence the intrinsic S—N bond energy should be less than that estimated by this system.

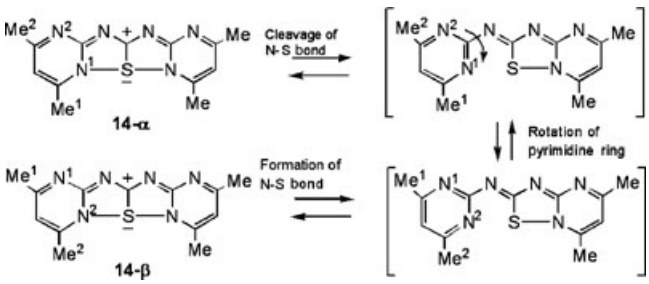

SCHEME 11 Rotation of the pyrimidine ring of **14**.

By using this system, the exchange energy of the two methyl groups can be measured separately for unsymmetrically substituted pyrimidine rings. As shown in Scheme 12, the exchange energy for Me^1 and Me^2 corresponds to the bond dissociation energy of N^1—S and that of Me^3 and Me^4 to that of S—N^3. Kinetic parameters obtained by variable temperature measurement of the rates are also shown in Table 1. The rate of exchange of Me^3 and

TABLE 1 Kinetic Parameters of Bond Cleavage of Pyrimidines

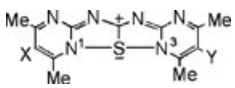

	X	*Y*		T_c (°C)	$\Delta G^{\ddagger}_{Tc}$ (kcal/mol)	$\Delta G^{\ddagger}_{298}$ (kcal/mol)	$\Delta H^{\ddagger}$ (kcal/mol)	ΔS (eu)
14	H	H		45	16.7	16.6	15.9 ± 1.1	-2.4 ± 3.4
15	Br	H	H-side	75	18.2	18.3	18.8 ± 0.3	1.8 ± 1.0
			Br-side	24	15.6	15.5	16.1 ± 1.3	2.2 ± 0.9

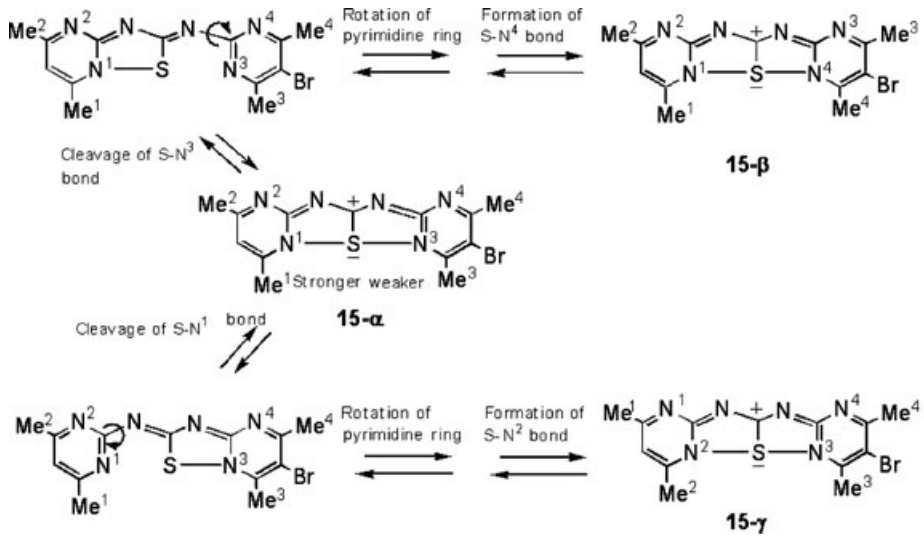

SCHEME 12 Rotation of the unsymmetrical pyrimidine of **15**.

Me^4 on the pyrimidine ring bearing an electron-withdrawing group (Br), i.e., exchange between **15-α** and **15-β**, is apparently faster and easier than that of Me^1 and Me^2 on the unsubstituted pyrimidine ring, i.e., exchange between **15-α** and **15-γ**. When we compare the $\Delta G^{\ddagger}_{298}$ for both processes, which for **15-α** and **15-β** is 15.5 kcal/mol and that for **15-α** and **15-γ** is 18.3 kcal/mol, the difference of $\Delta G^{\ddagger}_{298}$ is 2.8 kcal/mol. The average value (16.9 kcal/mol) is almost identical to that of the symmetrical molecule (**14**). The result clearly shows the labile character of the hypervalent bond and is deeply influenced ($\Delta\Delta G^{\ddagger}_{293} = 2.8$ kcal/mol) by a slight change of the electronegativity of the apical ligands (N^1 and N^3), which was effected by substitution by a bromine for a hydrogen (Table 1; Scheme 12).

EDGE INVERSION OF ANTIMONY(III) AND BISMUTH(III) COMPOUNDS

Although a variety of stable 10-S-3 sulfuranes had been prepared and their chemistry has been described, stable 10-P-3 compounds were first prepared by Arduengo et al. in 1984, as shown in Scheme 13 [24].

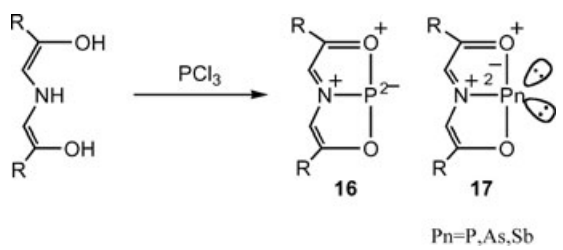

SCHEME 13 Synthesis of T-shaped 10-P-3 species.

The stability of this system is mainly based on two factors: (i) the molecule (**16**) is maintained neutral as a whole by the dicationic nature of the ligand and (ii) the cationic nature of the two apical oxygens strongly stabilizes the 3c-4e bond of 10-P-3. Arduengo and Dixon investigated electronic states of their 10-P-3 (**16**) system intensively by ab initio calculation. First they concluded that the electronic state of **16** is most accurately shown as **17**, where two pairs of unshared electrons reside on the central phosphorus atom just like thiathiophthene (**2**). When a saturated tridentate ligand is employed, planar structure can no longer be stable and the molecule (**18**) becomes pyramidal (8-P-3: **18a**) as shown in Scheme 14.

Based on the theoretical investigation of electronic state of **18**, it was proposed that the T-shaped structure of 8-P-3 compounds (**18b**) can be the transition state of inversion. This mechanism of inversion is called edge inversion. It is shown in Scheme 15 together with the well-known vertex inversion [25]. It is predicted that, at the transition state of edge inversion, a vacant p-orbital is present on the central atom perpendicularly to the molecular

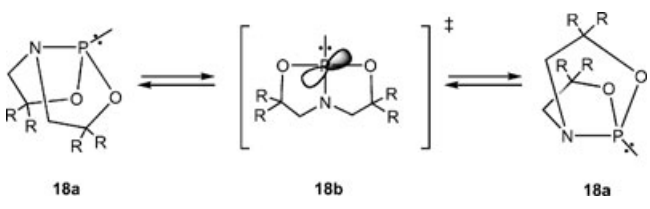

SCHEME 14 Inversion of **18** through T-shaped transition state.

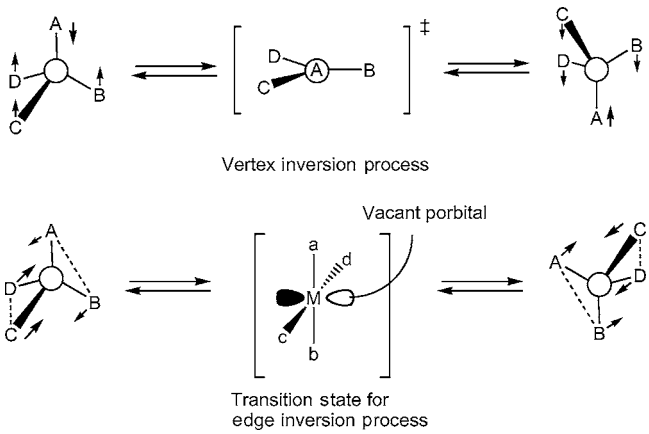

SCHEME 15 Mechanism of vertex inversion and edge inversion.

plane, and stereochemical identity of a pair of electrons is preserved as a ligand.

It is also concluded by ab initio calculation that the energy for edge inversion is decreased in contrast to that of vertex inversion according to (i) the increase of the size and of the electron-donating ability of the central atom and (ii) the decrease of the size and the increase of the electronegativity of substituents at the central atom (Table 2) [25–27].

Arduengo et al. experimentally showed that activation parameters for inversion of **18** (R,R = spiro(3,7)adamantyl) in toluene were $\Delta H^{\ddagger} = 23.4 \pm 1.6$ kcal/mol, $\Delta S^{\ddagger} = -1.2 \pm 4.2$ eu, which should be intramolecular because the activation entropy was nearly zero. The value of $\Delta H^{\ddagger}$ is clearly less than the vertex inversion barrier of 34.4 kcal/mol for PH_3 [28].

The inversion of this 8-P-3 compound bearing a saturated tridentate ligand should take place by edge inversion through a T-shaped intermediate (or TS: **18b**) according to the molecular design (Scheme 14).

TABLE 2 Calculated Energy Barrier of Vertax and Edge Inversion

	Vertax		*Edge*	
PH_3	35.0[a]	34.7[b]	159.9[a]	
AsH_3	41.3[a]	39.7[b]	142.2[a]	
SbH_3	42.8[a]	44.9[b]	112.2[a]	
BiH_3		60.5[b]		
PF_3	85.3[a]		53.8[a]	52.4[b]
AsF_3	66.3[a]		46.3[a]	45.7[b]
SbF_3	57.9[a]		38.7[a]	37.6[b]
BiF_3				33.5[b]

[a]From Dixon et al. [26] (MP2).
[b]From Moc and Morokuma [27] (MP2).

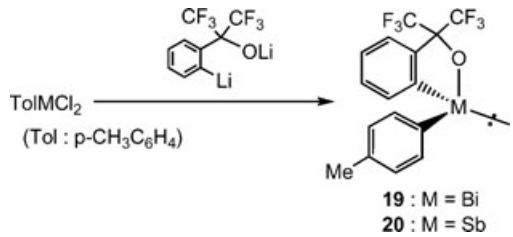

SCHEME 16 Synthesis of antimony(III) and bismuth(III) compounds.

Akiba and Yamamoto investigated the possibility of edge inversion recently by using a less sterically restricted model, where competition between edge inversion and vertex inversion can take place. Bismuth and antimony compounds (**19** and **20**) with a Martin ligand (hexafluorocumyl alcohol ligand) were prepared as shown in Scheme 16 [29]. There are two reasons to use a Martin ligand: (i) the ligand can stabilize organobismuth compounds that are usually not so stable thermally and (ii) the two CF_3 groups are anisochronous to the central atom. Thus, the inversion at the central atom can be observed as the exchange of the two CF_3 groups. However, the coalescence by the exchange of CF_3 group of neither bismuth compound (**19**) nor antimony (**20**) could be detected by ^{19}F NMR in nonnucleophilic solvents such as toluene and *o*-dichlorobenzene up to 150°C.

Another important aspect of edge inversion, that is, the appearance of vacant *p*-type orbital at the transition state perpendicularly to the molecular plane, was examined by the possibility of external nucleophile(s) to coordinate with the vacant *p*-type orbital of TS, thus lowering the energy of TS. Dixon and Arduengo predict that considerable stabilization of the TS should also be obtained by the second coordination of a nucleophile even after a large stabilization by the first one [30]. Then we prepared bismuth(III) (**21** and **22**) and antimony(III) compounds (**23** and **24**), each bearing one or two dimethylaminomethyl groups in the molecule that can coordinate to the central atom. The structures of **21–24** were determined by X-ray crystallography, and the rates of inversion were measured in several solvents as shown in Table 3. In nonnucleophilic solvents, the energy of inversion of bismuth compounds **19, 21**, and **22** decreased dramatically according to the increase of the number of intramolecular nucleophilic ligands. Coalescence temperatures (T_c) of **19, 21, 22** were above 175°C (*o*-dichlorobenzene), 125°C (toluene-d_8), and −90°C (dichloromethane), respectively. Also those in pyridine for **19** (T_c, 110°C) and **21** (T_c, 40°C) decreased significantly from those in nonnucleophilic solvents as mentioned above, but

TABLE 3 Kinetic Parameter of Edge Inversion of Bismuth and Antimony

Compound	*Solvent*	T_c (°C)	$\Delta G^{\ddagger}_{Tc}$ (kcal/mol)	$\Delta H^{\ddagger}$ (kcal/mol)	$\Delta S^{\ddagger}$ (eu)
19	*o*-Dichlorobenzene	$>175^a$	>21		
	Pyridine-d_5	110^a	18.0	9.0 ± 0.1	-23.5 ± 0.4
21	Toluene-d_8	125^b	20.5	12.8 ± 0.4	-18.8 ± 1.0
	Pyridine-d_5	40^a	14.6	7.1 ± 0.2	-23.6 ± 0.9
	2,6-Dimethylpyridine	170^a	20.6	12.4 ± 0.2	-18.6 ± 0.5
22	Dichloromethane-d_2	$< -90^a$	<8		
24	Dichloromethane-d_2	-55^a	9.4	9.3	−1.7

[a]By exchange of CF_3.
[b]By exchange of CH_2.

2,6-dimethylpyridine could not show this accelerating (coordinating) effect as expected based on steric hindrance of the molecule (Table 3).

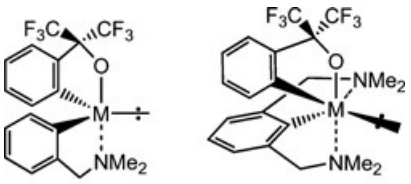

21 : M = Bi
23 : M = Sb

22 : M = Bi
24 : M = Sb

The strong coordination of an intramolecular ligand of dimethylamino group and also of an intermolecular nucleophilic solvent of pyridine to the TS was clearly shown by the fact that the activation free energy of **21** was 20.5 in toluene-d_8 and that in pyridine was 14.6 kcal/mol and the activation entropy was −18.8 and −23.6 eu. By measuring the coalescence of the methyl group of the dimethylamino group, the energy for cleavage of intramolecular Bi—N bond of **21** was determined to be 15.4 in toluene-d_8 and that in pyridine as 11.6 kcal/mol, which support the mechanism shown in Scheme 17 [29]. It is seen in Table 3 that the coordination of two pyridines for **19** and that of the dimethylamino group and one pyridine to **21** at TS gave almost identical activation entropy of −23 eu, and that the coordination of pyridine from the solvent lowered the activation enthalpy of **21** from 12.8 to 7.1 kcal/mol ($\Delta\Delta H^{\#} = 5.7$ cal/mol). The fact decisively exemplifies that the coordination of the second molecule of pyridine accelerates edge inversion significantly.

The inversion of bismuth compound **22** was too rapid to measure by ^{19}F NMR even at −90°C; hence, variable temperature NMR measurements were carried out for the corresponding antimony compound **24**. As expected, the rate of inversion of **24** was much slower than that of **22**; however, the activation free energy ($\Delta G^{\#}_{Tc}$) of **24** was very small, 9–10 kcal/mol

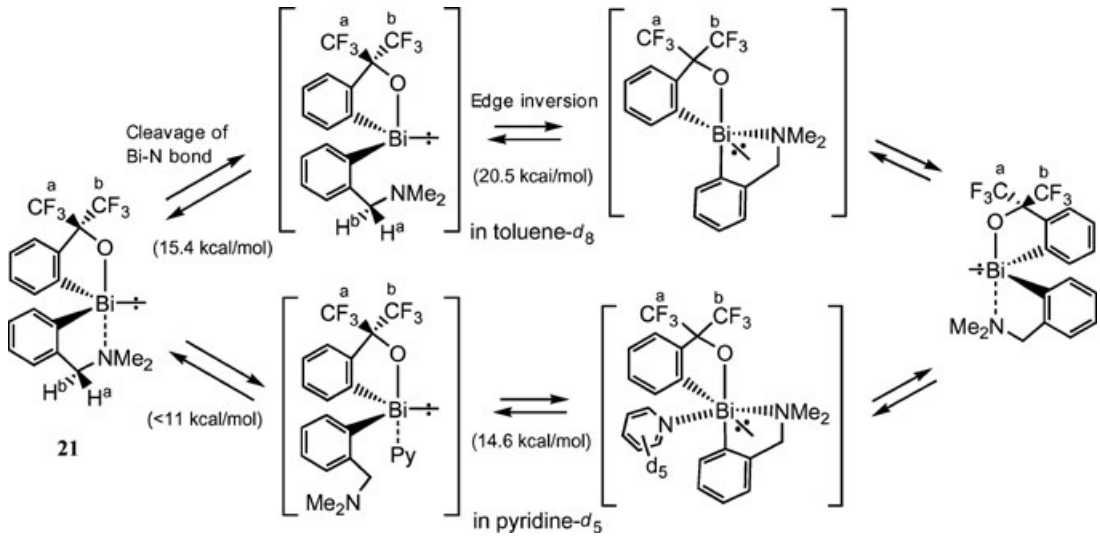

SCHEME 17 Energy diagram of edge inversion of **21** obtained from Table 3.

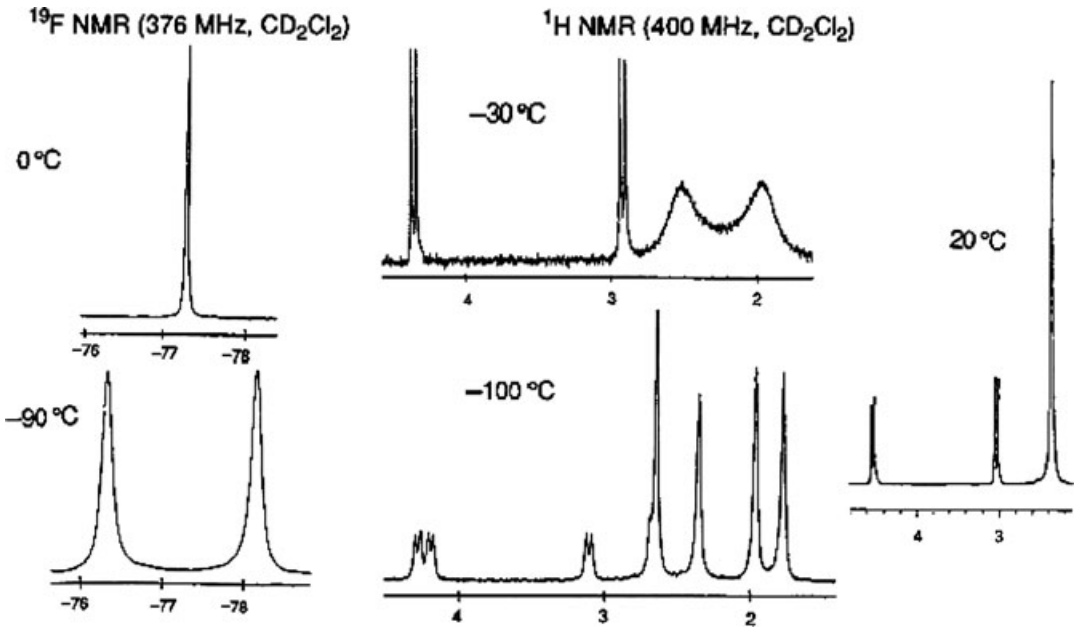

FIGURE 1 Temperature-dependent NMR spectra of edge inversion of **24**.

(Table 3). Two facts for **24** are essentially different from those for **19** and **21**: (i) the activation entropy was nearly zero and (ii) there was no effect of nucleophilic solvent (pyridine) on the rate. These strongly support the proposal that the inversion at the antimony of **24** is effected by the intramolecular coordination of the two dimethylamino groups to the vacant *p*-type orbital at TS, thus generating a typical 3c-4e bond at the TS. The bond dissociation energy of Sb—N bond of **24** was obtained by the exchange of the two anisochronous methyl groups of NMe_2 as 12.0 kcal/mol. This is clearly much larger than the activation energy of inversion; hence, it is certain that the two Sb—N bonds are not dissociated at all during the inversion.

From the NMR spectra shown in Fig. 1, the following three facts are apparent: (i) at around −100°C, there are two quartets of CF_3 groups and four methyl groups and two sets of CH_2 two doublets that correspond to the solid-state structure of **24**; (ii) at −30°C, four methyl groups coalesce to two groups and two sets of CH_2 two doublets to one set of two doublets; (iii) at 20°C, there can be seen only one signal for the methyl, methylene, and trifluoromethyl group. ORTEP drawings of **22** and **24** and the movement of the molecule during edge inversion are shown in Scheme 18.

The important results that the above-mentioned inversion was very much accelerated by the coordination of two nucleophilic substituents and that the rate of inversion of bismuth compound **22** was much faster than that of antimony compound **24** are consistent with the prediction of an edge inversion mechanism.

As the inversion of bismuth compound **19** was too slow to measure by the coalescence of the two CF_3 groups, one of the CF_3 groups was replaced by a CH_3 group in order to have a chiral carbon in the ligand of bismuth compound **25**. Thus, diastereomers of **25** were separated and the barriers of inversion were obtained from the rates of equilibration of the diastereomers. The inversion rate of **25** in 1,2-dichloroethane was faster when *p*-substituent of benzene ring is π-donative (**25a**) or σ-attractive (**25b**) compared to the methyl group (**25c**): **25a** > **25b** > **25c**. This is also consistent with what is expected from the edge inversion mechanism [29].

Arduengo et al. have already investigated the inversion at the germanium atom of **26** and concluded that the inversion proceeds by the edge inversion mechanism [30]. Thus, there is a good possibility for the edge inversion mechanism to be operative generally for heavier main group compounds even without lone-pair electrons.

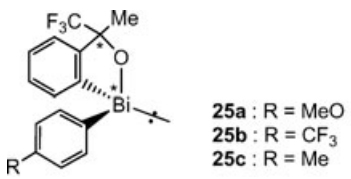

25a : R = MeO
25b : R = CF_3
25c : R = Me

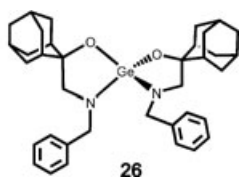

26

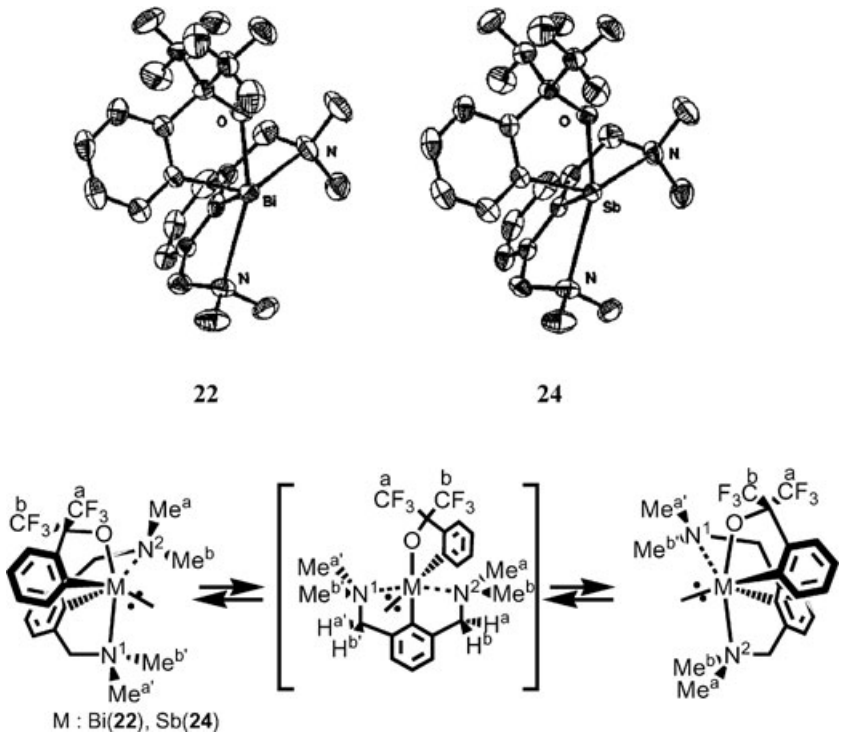

SCHEME 18 ORTEP drawing and the movement of **22** and **24** during edge inversion.

SYNTHESIS, STRUCTURES, AND BOND SWITCHING OF BORON COMPOUNDS BEARING 1,8-BIS(DIMETHYLAMINO) ANTHRACENE SKELETON

X-ray crystallographic analysis of boron compounds bearing the 1,8-bis(dimethylamino)anthracene skeleton (Fig. 2) showed unsymmetrical structures with coordination of only one NMe_2 group toward the central boron atom. Shorter N—B bond lengths are 1.809(2) Å in **27**, 1.739(2) Å in **28**, and 1.664(3) Å in **29**, and the longer N—B bonds are 2.941(2) Å in **27**, 3.124(3) Å in **28**, and 3.129(3) Å in **29**. The average of N—B—N distances is 4.80 Å [31].

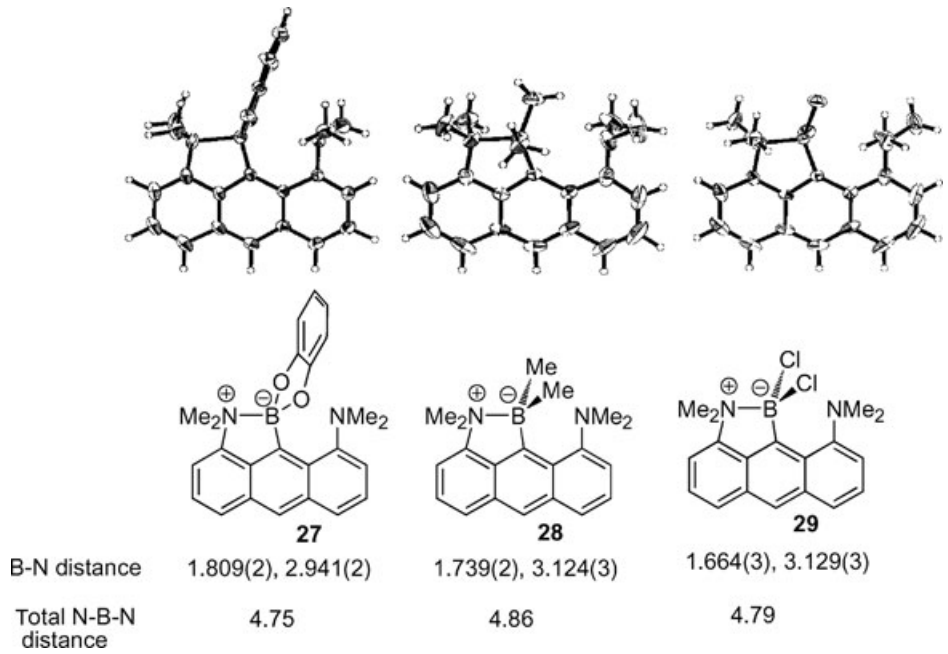

FIGURE 2 ORTEP drawing and B—N bond distances of **27–29**.

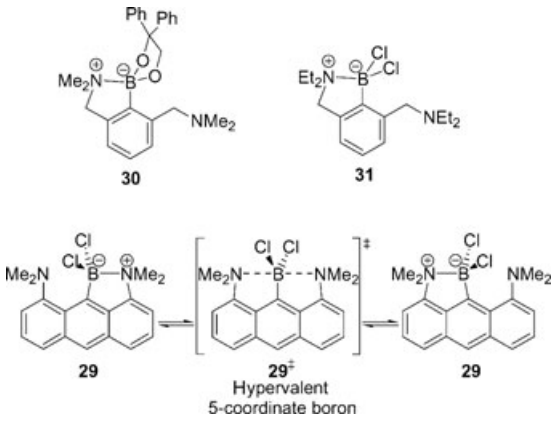

SCHEME 19 Very rapid N–B bond switching equilibration of **29**.

The energy difference between the unsymmetrical tetracoordinate structure and the symmetrical pentacoordinate one, however, should be very small based on the variable temperature ^{1}H NMR measurement. The NMR spectra ($CDCl_3$ or CD_2Cl_2) of **27–29** showed symmetrical anthracene patterns in the aromatic region (two kinds of doublets, a triplet, and a singlet) and a sharp singlet signal of the methyl group for the two NMe_2 groups at room temperature. The peaks maintained their sharpness and the symmetrical pattern even at −80°C. This is the case even in the most unsymmetrical dichloro compound **29** (CD_2Cl_2). It was similar to the behavior of **30** in ^{1}H NMR, which showed only one singlet (12H) of the two NMe_2 groups and maintained its sharpness in CD_2Cl_2 from 25°C to −100°C [32]. However, it is contrasted with the behavior of BCl_2[2,6-$(Et_2NCH_2)_2C_6H_3$] (**31**) in ^{1}H NMR, which showed two kinds of NEt_2 groups in C_6D_6 or THF-d_8 solvents at 25°C [33]. The NMR data of **29** indicate that the very rapid "bond switching" accompanied with the inversion at the central boron atom [31,34] is taking place in solution as illustrated in Scheme 19. Since the energy barrier of the N—B bond-switching process in **29** was too small to measure by the coalescence method, the energy difference between the unsymmetrical tetracoordinate dichloroboron **29** and the pentacoordinate one **29**‡, which should be the transition state of the bond-switching process, must be very small. The small activation energy in **29** indicates that our newly prepared rigid anthracene ligand system stabilizes the pentacoordinate dichloroboron transition state (**29**‡), where 3c-4e bond should be formed.

In tetracoordinate boron compounds (**27–29**), the average of shorter B—N length (B^1—N^1: 1.737 Å) is 10% longer than the sum of the covalent radius of boron and nitrogen (1.738 Å; (0.88 + 0.70) × 1.10) [35]; on the other hand, the average of longer B—N length (B^1—N^2: 3.065 Å) apparently coincides with 10% longer distance of the sum of van der Waals radius of boron and covalent radius of nitrogen (3.058 Å; (2.08 + 0.70) × 1.10). These distances indicate that one of two NMe_2 groups interacts strongly to make a shorter B—N bond with the central boron atom, and the other one interacts very weakly to make a longer B—N bond with the central boron atom.

The bond-switching situation is schematically illustrated in Fig. 3. The blue and black circles at the left-hand side of (A) show the shorter N—B bond where the radii of nitrogen N^1 and boron B^1 are elongated 10% of each covalent radius amounting to 1.74 Å, which coincides with the average bond length of the shorter B—N bond of **27–29**. The blue circle at the right-hand side of N^2 shows the weakly interacting nitrogen, the radius should be in between the covalent radius (0.70 Å) and 10% longer one (0.77 Å), because the radius of N^2 shall be slightly (a few percent) longer than the regular covalent radius based on the weak interaction with $\sigma*_{N1-B1}$. The distance between the two nitrogens is 4.80 Å, which is the same as the average of experimental values of **27–29**.

When the interaction between B^1 and N^2 comes into play, B^1 moves to $B^{1\prime}$ gradually, and the radius of N^2 becomes gradually enlarged up to 10% from the covalent radius to build a new $B^{1\prime}$—N^2 bond and that of N^1 shall be compressed nearly to the covalent radius, which are shown by dotted circles. Hence, the boron in the middle moves back and forth rapidly as a piston rod in the range of 1.32 Å (4.80 − 2 × 1.74), being connected to the carbon of C-9 of anthracene skeleton. The length of the arm (B^1—C^9: 1.622 Å) is the same as the sum of covalent radius of sp^2 carbon (0.74 Å) and the boron (0.88 Å). The length of the arm stays normal and is not elongated at all. Here, C^1 and C^8 of anthracene skeleton are bound to N^1 and N^2.

The distance (3.06 Å) between B^1 and N^2 coincides exactly with the sum of 10% longer distance of van der Waals radius of the central boron and the covalent radius of nitrogen. This coincidence involves quite interesting and meaningful chemical view that a covalent interaction in the frontside and van der Waals interaction at the backside reside on the central boron atom; this image should correspond to an early stage of S_N2 reaction as shown in Fig. 3(B). In other words, a pair of electrons moves back and forth on a linear line of 3c-4e bond of N—B···N, just like the movement of a piston rod accompanied by the inversion of stereochemistry at the boron, that is bond switching. This movement of a pair of electrons does not involve any kind of a curved movement of electrons, which a term like bell-clapper

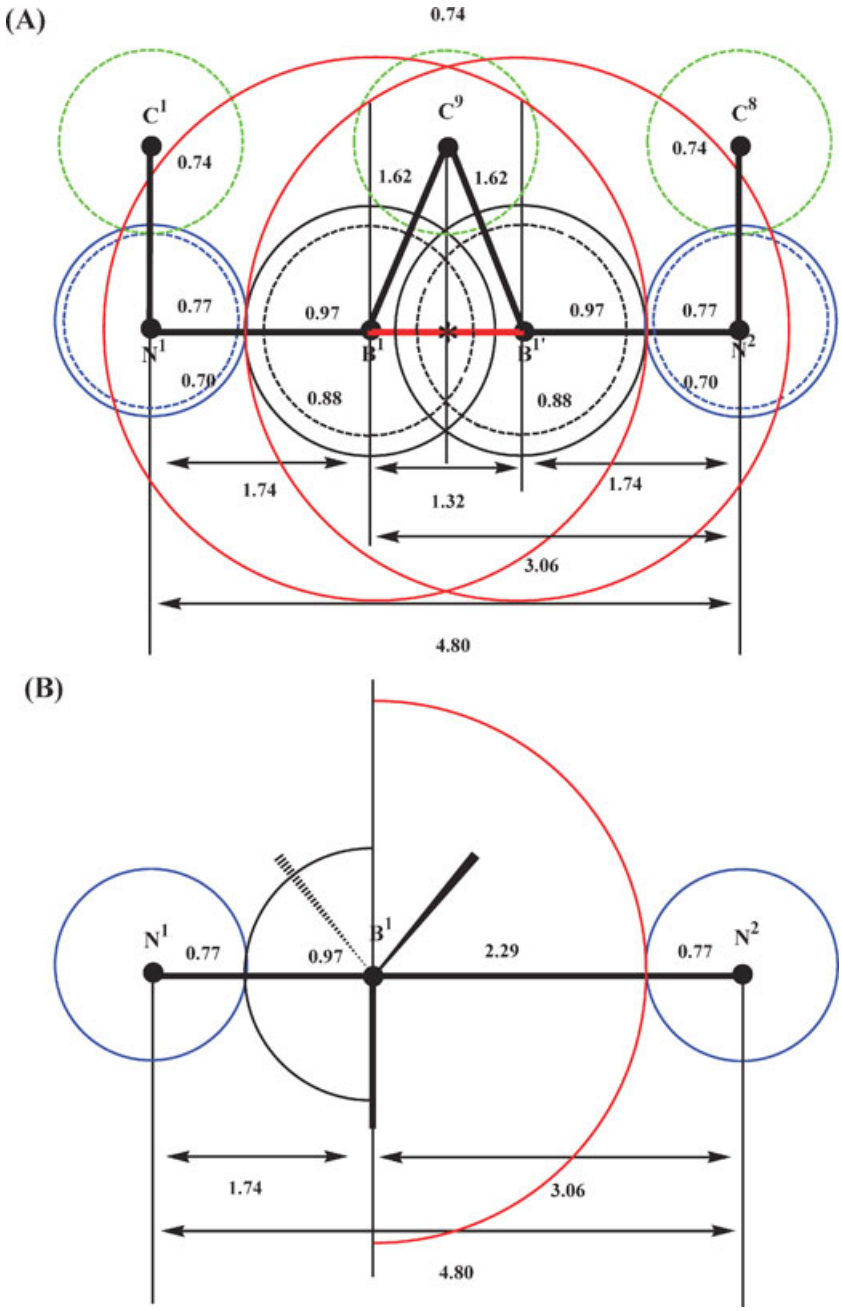

FIGURE 3 Diagram of bond switching of N—B···N on anthracene skeleton of **27–29**. Circle: 110% of covalent radius; blue (N, 0.77), black (B, 0.97). Circle (red): 110% of van der Waals radius of boron (B, 2.29). Dotted circle: covalent radius; blue (N, 0.70), black (B, 0.88), green ($C_{(sp2)}$, 0.74). Numerical values in parentheses are in angstroms.

rearrangement or pendulum motion let us imagine.

This rationalization should certainly be applicable to the movement of the central sulfur in Scheme 10 and also to the bond cleavage and formation in Schemes 11and 12. This type of dynamic movement of the central carbon atom in 10-C-5 species could not be observed by ^{1}H NMR measurement because of almost symmetric nature of 10-C-5 species [31,36].

In conclusion, we have presented a variety of reactions and equilibrations rationalized as the effect of 10-S-3, edge inversions of antimony(III) and bismuth(III) as that of 12-M-5, and also bond-switching equilibrations (eternal S_N2) effected by covalent interactions of nitrogen and boron atoms as that of

10-B-5. In all of these, the formation of 3c-4e bond of heteroatoms acts as the central feature.

REFERENCES

[1] Akiba, K.-y. Chemistry of Hypervalent Compounds; Akiba, K.-y. (Ed.); Wiley-VCH: Weinheim, Germany, 1999; Ch. 1 and 2.

[2] Chui, C.; Corriu, R. J. P. Chemistry of Hypervalent Compounds; Akiba, K.-y. (Ed.); Wiley-VCH: Weinheim, Germany, 1999; Ch. 4; Kira, M.; Zhang, L. C. ; Akiba, K.-y. (Ed.); Wiley-VCH: Weinheim, Germany, 1999; Ch. 5.

[3] Kawashima, T. Chemistry of Hypervalent Compounds; Akiba, K.-y. (Ed.); Wiley-VCH: Weinheim, Germany, 1999; Ch. 6.

[4] (a) Furukawa, N.; Sato, S. Chemistry of Hypervalent Compounds, Akiba, K.-y. (Ed.); Wiley-VCH; Weinham, Germany, 1999; Ch. 8; (b) Lenz, D.; Seppelt, K.; Akiba, K.-y. (Ed.); Wiley-VCH: Weinheim, Germany, 1999; Ch. 10.

[5] (a) Zhdankin, V. V.; Stang, P. J. Chemistry of Hypervalent Compounds; Akiba, K.-y. (Ed.); Wiley-VCH: Weinham: Germany, 1999; Ch. 11; (b) Ochiai, M.; Akiba, K.-y. (Ed.); Wiley-VCH: Weinheim, Germany, 1999; Ch. 12.

[6] (a) Pimentel, G. C. J Chem Phys 1951, 19, 446; (b) Hackland, R. J.; Rundle, R. E. J Am Chem Soc 1951, 73, 4321.

[7] Musher, J. I. Angew Chem, Int Ed 1969, 8, 54.

[8] (a) Kutzelnigg, W. Angew Chem, Int Ed 1984, 23, 272 and references therein; (b) Reed, A. E.; Schleyer, P. v. R. J Am Chem Soc 1990, 112, 1434 and references therein.

[9] (a) Bezzi, S.; Mammi, M.; Garbuglio, C. Nature 1958, 182, 247; (b) Lozac'h, N. Adv Heterocyclic Chem 1971, 13, 161; (c) Hansen, L. K.; Hordvik, A. Acta Chem Scand 1973, 27, 411; (d) Hordvik, A.; Seathre, L. J. Acta Chem Scand 1972, 26, 3114.

[10] Kingsberg, E. Q Rev 1969, 23, 537.

[11] (a) Behringer, H.; Bender, D.; Falkenberg, J.; Wiedenmann, R. Chem Ber 1968, 101, 1423; (b) Behringer, H.; Wiedenmann, R. Tetrahedron Lett 1965, 3705.

[12] Lang, G.; Vialle, J. Bull Soc Chim Fr 1967, 2865.

[13] (a) Easton, D. B.; Leaver, D. Chem Commun 1965, 585; (b) Lakshmikantham, M. V. J Org Chem 1976, 41, 879.

[14] (a) Akiba, K.-y.; Tsuchiya, T.; Inamoto, N. Tetrahedron Lett 1976, 1877; (b) Akiba, K.-y.; Ochiumi, M.; Tsuchiya, T.; Inamoto, N. Tetrahedron Lett 1975, 459.

[15] Yamamoto, Y.; Tsuchiya, T.; Ochiumi, M.; Arai, S.; Inamoto, N.; Akiba, K.-y. Bull Chem Soc Jpn 1989, 62, 211.

[16] (a) Akiba, K.-y.; Arai, S.; Tsuchiya, T.; Yamamoto, Y.; Iwasaki, F. Angew Chem, Int Ed 1979, 18, 166 and references therein; (b) Iwasaki, F.; Akiba, K.-y. Acta Crystallogr, Sect B: Struct Sci 1981, 37, 180.

[17] (a) Akiba, K.-y.; Kobayashi, T.; Arai, S. J Am Chem Soc 1979, 101, 5857; (b) Iwasaki, F.; Akiba, K.-y. Acta Crystallogr, Sect B: Struct Sci 1981, 37, 185.

[18] Yamamoto, Y.; Akiba, K.-y. J Am Chem. Soc 1984, 106, 2713.

[19] Yamamoto, Y.; Akiba, K.-y. Bull Chem Soc Jpn 1989, 62, 479.

[20] (a) Akiba, K.-y.; Kashiwagi, K.; Ohyama, Y.; Yamamoto, Y.; Ohkata, K. J Am Chem Soc 1985, 107, 2721; (b) Ohkata, K.; Ohyama, Y.; Watanabe, Y.; Akiba, K.-y. Tetrahedron Lett 1984, 25, 4561.

[21] (a) Iwasaki, F.; Akiba, K.-y. Bull Chem Soc Jpn1984, 57, 2581; (b) Hordvik, A.; Julsham, K. Acta Crystallogr, Sect A: Found Crystallogr 1981, 31, 292.

[22] (a) Ohkata, K.; Ohsugi, M.; Iwasaki, H.; Akiba, K.-y. J Am Chem Soc 1988, 110, 5576; (b) Ohkata, K.; Ohsugi, M.; Yamamoto, K.; Ohsawa, M.; Akiba, K.-y. J Am Chem Soc 1996, 118, 6355.

[23] (a) Ohkata, K.; Ohsugi, M.; Kuwaki, T.; Yamamoto, K.; Akiba, K.-y. Tetrahedron Lett 1990, 31, 1605; (b) Ohkata, K.; Yamamoto, K.; Ohsugi, M.; Ohsawa, M.; Akiba, K.-y. Heterocycles 1994, 37, 1707.

[24] (a) Culley, S. A.; Arduengo, A. J., III. J Am Chem Soc 1984, 106, 1164; 1985, 107, 1089; (b) Stewart, C. A.; Harlow, R. L.; Arduengo, A. J., III. J Am Chem Soc 1985, 107, 5543.

[25] (a) Dixon, D. A.; Arduengo, A. J., III. J Am Chem Soc 1986, 108, 2461; (b) Dixon, D. A.; Arduengo, A. J., III. J Chem Phys 1987, 91, 3195.

[26] Dixon, D. A.; Arduengo, A. J., III; Fukunaga, T. J Am Chem Soc 1987, 109, 338.

[27] Moc, J.; Morokuma, K. Inorg Chem 1994, 33, 551.

[28] Arduengo, A. J., III; Dixon, D. A.; Roe, D. C. J Am Chem Soc 1986, 108, 6821.

[29] (a) Yamamoto, Y.; Chen, X.; Akiba, K.-y. J Am Chem Soc 1992, 114, 7906; (b) Yamamoto, Y.; Chen, X.; Kojima, S.; Ohdoi, K.; Kitano, M.; Doi, Y.; Akiba, K.-y. J Am Chem Soc 1995, 117, 3922.

[30] (a) Dixon, D. A.; Arduengo, A. J., III. Int J Quantum Chem Symp 1988, 22, 85; (b) Arduengo, A. J., III; Dixon, D. A.; Roe, D. C.; Kline, M. J Am Chem Soc 1988, 110, 4437.

[31] Yamashita, M.; Yamamoto, Y.; Akiba, K.-y.; Hashizume, D.; Iwasaki, F.; Takagi, N.; Nagase, S. J Am Chem Soc 2005, 127, 4354.

[32] Toyota, S.; Futawaka, T.; Ikeda, H.; Oki, M. J Chem Soc, Chem Commun 1995, 2499.

[33] Schlengerman, R.; Sieler, R.; Hey-Hawkins, E. Main Group Chem 1997, 2, 141.

[34] (a) Forbus, T. R., Jr.; Martin, J. C. J Am Chem Soc 1979, 101, 5057; (b) Martin, J. C. Science 1983, 221, 509; (c) Martin, J. C. et al. Heteroatom Chem 1993, 4, 113; 4, 129, 137.

[35] Dean, J. A. Lange's Handbook of Chemistry, 11th ed.; McGraw-Hill: New York, 1973; p. 119.02.

[36] (a) Akiba, K.-y.; Moriyama, Y.; Mizozoe, M.; Inohara, H.; Nishii, T.; Yamamoto, Y.; Minouta, M.; Hashizume, D.; Iwasaki, F.; Takahi, N.; Ishimura, K.; Nagase, S. J Am Chem Soc 2005, 127, 5893; (b) Akiba, K.-y.; Yamashita, M.; Yamamoto, Y.; Nagase, S. J Am Chem Soc 1999, 121, 10644.